

Effect of a in-plane magnetic field on the microwave assisted magnetotransport in a two-dimensional electron system

Jesús Iñarrea^{1,2} and Gloria Platero²

¹*Escuela Politécnica Superior, Universidad Carlos III, Leganes, Madrid, Spain and*

²*Unidad Asociada al Instituto de Ciencia de Materiales, CSIC, Cantoblanco, Madrid, 28049, Spain.*

(Dated: March 9, 2022)

In this work we present a theoretical approach to study the effect of an in-plane (parallel) magnetic field on the microwave-assisted transport properties of a two-dimensional electron system. Previous experimental evidences show that microwave-induced resistance oscillations and zero resistance states are differently affected depending on the experimental set-up: two magnetic fields (two-axis magnet) or one tilted magnetic field. In the first case, experiments report a clear quenching of resistance oscillations and zero resistance states. In a tilted field, one obtains oscillations displacement and quenching but the latter is unbalanced and less intense. In our theoretical proposal we explain these results in terms of the microwave-driven harmonic motion performed by the electronic orbits and how this motion is increasingly damped by the in-plane field.

PACS numbers:

In recent years, with the rise of Nanotechnology, a lot of effort has been devoted to the study and research of physics of nano-devices, from theoretical, experimental and application perspectives. In particular the response of such systems to external, time-dependent or stationary, fields is receiving much attention from the scientific community¹. A remarkable example is the recently obtained microwave- (MW-) induced resistance oscillations (MIRO) and zero resistance states (ZRS)²⁻⁴ in two-dimensional electron system (2DES). These striking results have been the subject of intense current interest in the condensed matter community.

Thus, new experimental evidences are being published in a continuous basis challenging the available theoretical models⁵⁻¹¹. Among all of those experimental outcomes we can cite for instance, temperature dependence of MIRO^{2,3,5}, absolute negative conductivity¹²⁻¹⁴, bichromatic MW excitation^{15,16}, polarization immunity of magnetoresistance (ρ_{xx})¹⁷⁻¹⁹ and the effect of MW frequency on MIRO and ZRS^{20,21}. An important set of results on MIRO that has not received yet special attention from theorists is the effect of an in-plane magnetic field (B_{\parallel}) (parallel to the 2DES, x-y plane) on the transport properties of these devices. In a two-axis magnet experiment, we have two magnetic fields: B_{\parallel} and the magnetic field perpendicular (B_{\perp}) to the 2DES²². In a tilted magnetic field (B_{tilted}) experiment, we only have one field and in this case B_{\parallel} is the parallel component of B_{tilted} ²³. In the first case²² (Yang's experiment) results show an strong suppression of MIRO and ZRS. The second case²³ (Mani's experiment) demonstrates a displacement of MIRO at larger B_{tilted} and an unbalanced quenching. Therefore these unexpected results deserve to be considered by the different theoretical approaches serving as a crucial test for them.

In this paper we present a theoretical model to address those results and try to reconcile them using a common physical mechanism. When a 2DES is illuminated with MW radiation, electronic orbits are forced to move back and forth, oscillating harmonically at the frequency of MW radiation and with an amplitude proportional to the MW electric field^{5,14}. MIRO are proportional to the magnitude of this amplitude and any variation of it, is finally reflected on MIRO. In their MW-driven orbits motion, electrons interact with the lattice ions being damped and producing acoustic phonons. According to our model, the presence of B_{\parallel} imposes an extra harmonically oscillating motion in the z -direction enlarging the electrons trajectory in their orbits. This would increase the interactions with the lattice making the damping process more intense and reducing the amplitude of the orbits

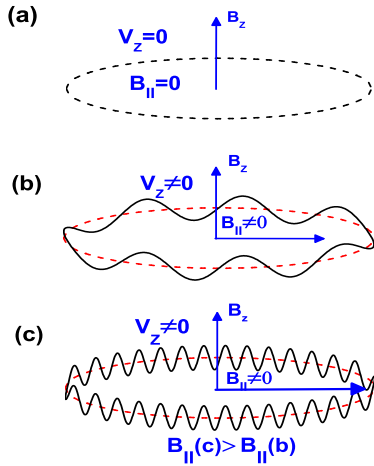


FIG. 1: Schematic diagrams showing the semiclassical description of electron trajectories in 2D systems under different potentials and fields. 1(a): 2D ($x - y$ plane) parabolic potential. 1(b) and 1(c): 2D + 1D parabolic potentials and an in-plane magnetic field B_{\parallel} .

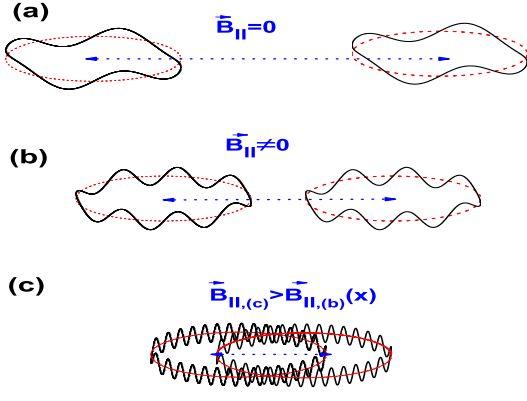


FIG. 2: Schematic diagram showing the dependence of MW-driven electronic orbit oscillating motion with B_{\parallel} . From (a) to (c), B_{\parallel} intensity increases which makes the MW-driven amplitude smaller and smaller. Eventually the oscillating motion collapses, amplitude goes to zero and MIRO are quenched.

oscillations. However depending on the origin of B_{\parallel} , the damping intensity would be different. Thus, in Yang's experiment²² the magnetic fields B_{\parallel} and B_{\perp} are not related and B_{\parallel} is kept constant while B_{\perp} increases from zero. Thus, the effect of B_{\parallel} is the same in the whole ρ_{xx} response and MIRO are uniformly quenched. However in Mani's experiment B_{\parallel} would not be constant because depends on B_{tilted} . Then the quenching of MIRO would be unbalanced and only visible at larger values of B_{tilted} .

The Hamiltonian for electrons confined in a 2D system (x - y plane) by a potential $V(z)$ and subjected to a magnetic field $B = (B_x, 0, B_z)$, ($B_{\parallel} = B_x$ and $B_{\perp} = B_z$) is given by :

$$\begin{aligned} H_0 &= \frac{P_x^2 + P_y^2}{2m^*} + \frac{w_z}{2}L_z + \frac{1}{2}m^* \left[\frac{w_z}{2} \right]^2 (x^2 + y^2) \\ &+ \frac{P_z^2}{2m^*} + \frac{1}{2}m^*w_z^2z^2 + V(z) + \frac{1}{2}w_xz(exB_z - 2P_y) \\ &= H_{xy} + H_z + \frac{1}{2}w_xz(exB_z - 2P_y) \end{aligned} \quad (1)$$

We have used the symmetric gauge for B_z : $\vec{A}_{B_z} = -\frac{1}{2}\vec{r} \times \vec{B} = (-\frac{y}{2}B_z, \frac{x}{2}B_z, 0)$, and the Landau gauge for B_x : $\vec{A}_{B_x} = (0, -zB_x, 0)$. w_z is the cyclotron frequency of B_z : $w_z = \frac{eB_z}{m^*}$ and w_x of B_x : $w_x = \frac{eB_x}{m^*}$. L_z is the z -component of the electron total angular momentum. According to the experimental parameters used^{22,23} the hamiltonian term $\frac{1}{2}w_xz(exB_z - 2P_y) \ll H_{xy} + H_z$. Then, we can discard this term and write: $H_0 \simeq H_{xy} + H_z$.

When one considers a parabolic potential for $V(z)$: $V(z) = \frac{1}{2}m^*w_0^2z^2$, the Hamiltonian H_z can finally be written as:

$$H_z = \frac{P_z^2}{2m^*} + \frac{1}{2}m^*(w_x^2 + w_0^2)z^2 = \frac{P_z^2}{2m^*} + \frac{1}{2}m^*\Omega^2z^2 \quad (2)$$

and the Schrodinger equation of H_0 can directly be solved. We obtain the wave functions of two harmonic

oscillators, one is two-dimensional in the $x - y$ plane and the other one is one-dimensional in the z -direction. In a semiclassical approach the electron is subjected simultaneously to two independent harmonic motions with a trajectory depicted in Figure 1: the electron performs a circular movement in the $x - y$ plane and at the same time a 1D harmonic oscillating motion in the z direction. In Fig. 1(a) we present the semiclassical trajectory of an electron in a 2D parabolic potential: the electron trajectory is circular. In Fig. 1(b) and 1(c), we add a parabolic potential in the z direction, then the electron trajectory is circular in the plane and at the same time is oscillating in z . We introduce also B_{\parallel} and the oscillations in z direction increase with the intensity of B_{\parallel} . We obtain similar results when $B_{\parallel} = B_y$.

The problem of two-dimensional electrons subjected to magnetic fields at arbitrary angles has been already solved analytically with a parabolic confinement in the perpendicular direction^{24,25}. According to these results the Hamiltonian can be transformed through a rotation of the coordinate system with a certain angle. The obtained Hamiltonian corresponds to two Hamiltonians of quantum harmonic oscillators and can be exactly solved^{24,25}.

If now we switch on the MW radiation (plane-polarized in the x -direction) and connect a constant electric field (E_{dc}) in the same direction (transport direction) the Hamiltonian then reads:

$$\begin{aligned} H_T &= \frac{P_x^2 + P_y^2}{2m^*} + \frac{w_z}{2}L_z + \frac{1}{2}m^* \left[\frac{w_z}{2} \right]^2 [(x - X)^2 + y^2] \\ &- \frac{1}{2}eE_{dc}X - eE_0(x - X) \cos wt - eE_0X \cos wt \\ &+ \frac{P_z^2}{2m^*} + \frac{1}{2}m^*\Omega^2z^2 \end{aligned} \quad (3)$$

X is the center of the orbit for the electron spiral motion: $X = \frac{eE_{dc}}{m^*(w_c/2)^2}$. The corresponding time-dependent Schrodinger equation can be exactly solved^{5,14,16} and the wave functions are:

$$\Psi_T(x, y, t) \propto \phi_N [(x - X - a(t)), (y - b(t)), t] \phi(z) \quad (4)$$

where ϕ_N are Fock-Darwin states²⁶ and $\phi(z)$ is the one-dimensional harmonic oscillator wave function. $a(t)$ (for the x -coordinate) and $b(t)$ (for the y -coordinate) are the solutions for a classical driven 2D harmonic oscillator. The expression, for instance, for $a(t)$ ¹⁸ is:

$a(t) = \frac{eE_0}{m^*\sqrt{(w_z^2 - w^2)^2 + \gamma^4}} \cos wt = A \cos wt$, where E_0 is the amplitude of the MW electric field, w the frequency and e the electron charge. γ is a damping factor which dramatically affects the movement of the MW-driven electronic orbits. Along with this movement interactions occur between electrons and lattice ions, yielding acoustic phonons and producing a damping effect in the electronic motion. In Ref.^{5,21}, we developed a microscopical model to calculate γ . We obtained that γ is a material and sample-dependent parameter which depends also

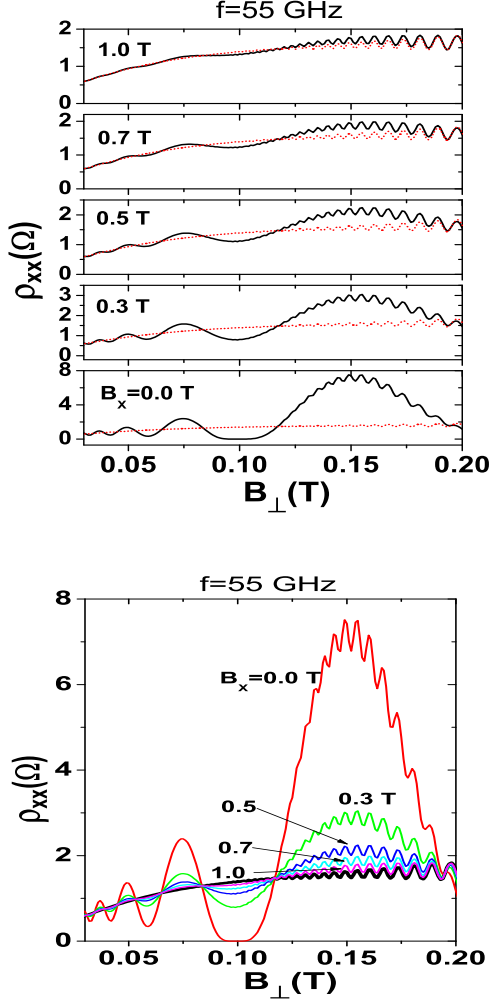


FIG. 3: Calculated results of ρ_{xx} vs B_{\perp} for different values of B_x from 0.0 T to 1.0 T. B_{\perp} and B_x are independent. In the top panel we present the curves of each value of B_x in individual panels. Single lines correspond with MW on, and dotted lines with MW off. We observe a progressive quenching of ρ_{xx} oscillations as B_x increases. In the bottom panel we present all curves together for comparison. MW frequency is 55 GHz. $T=1K$.

on lattice temperature, electronic orbit length and MW frequency^{5,21}. As we have indicated above, in a semiclassical explanation the presence of B_{\parallel} alters the electron trajectory in its orbit increasing the frequency and the number of oscillations in the z -direction. Now the frequency of the z -oscillating motion is $\Omega > w_0$. This makes longer the electron trajectory increasing the total orbit length and eventually the damping. This increase in the orbit length is proportionally equivalent to the increase in the number of oscillations in the z -direction. Thus, we introduce the ratio of frequencies after and before connecting B_{\parallel} as a correction factor for the damping factor

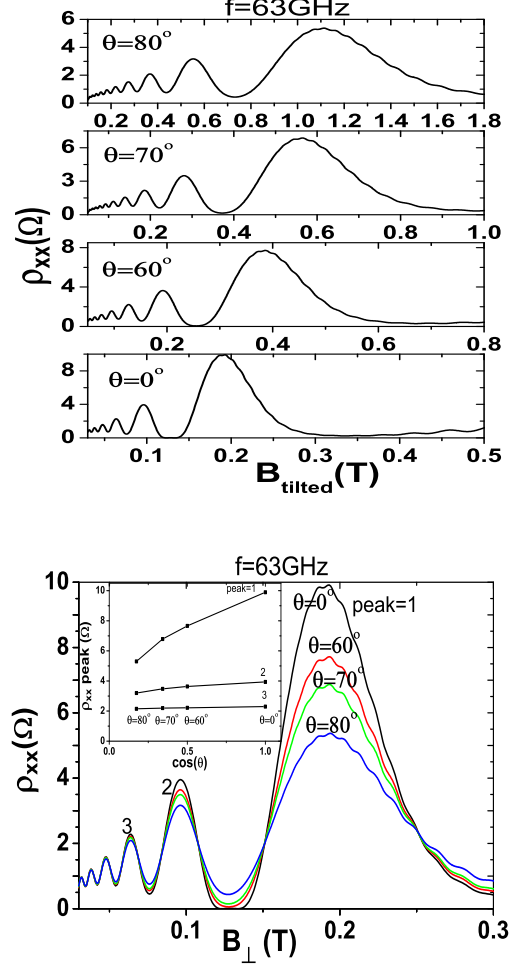


FIG. 4: Calculated results of ρ_{xx} vs B_{tilted} for different values of θ . In the top panel we present the curves of each value of θ in individual panels. In the bottom panel we present all curves together for comparison vs B_{\perp} . MW frequency is 63 GHz. In the inset we present the peak resistance vs $\cos \theta$. $T=1K$.

γ . The final damping parameter γ_f is:

$$\gamma_f = \gamma \times \frac{\Omega}{w_0} = \gamma \times \sqrt{1 + \left(\frac{w_x}{w_0}\right)^2} = \gamma \times \sqrt{1 + \left(\frac{eB_x}{m^*w_0}\right)^2} \quad (5)$$

Now, following a previous model developed by us^{5,14}, we are able to calculate ρ_{xx} , resulting that is proportional to the MW-induced oscillation amplitude of the electronic orbits center:

$$\rho_{xx} \propto A \cos w\tau = \frac{eE_o}{m^* \sqrt{(w_z^2 - w^2)^2 + \gamma_f^4}} \cos w\tau \quad (6)$$

where τ is the charged impurity scattering time^{5,14}. In Figure 3 we present calculated results of ρ_{xx} vs B_{\perp} for

different values of B_x being B_x independent of B_\perp as in Yang's experiment. Thus, calculations have been made for a MW frequency of 55 GHz and a confinement in z of 50 nm (similar as Yang's experiment). B_x values are: $B_x(T) = 0.0, 0.3, 0.5, 0.7$ and 1.0 . In the top panel we can see the results for each value of B_x in individual panels. We observe clearly the progressive quenching of MIRO as B_x increases. In the bottom panel we present all curves together in the same panel for comparison. According to equations (5) and (6), when we increase B_x , we also increase the damping γ_f and as a result the amplitude A and MIRO are progressively quenched. We obtain a total quenching for $B_x \simeq 1.0$ T. We observe a uniform damping in the whole range of B_\perp for each value of B_x . These results are in good agreement with experiment²². In Figure 4 we present calculated results of ρ_{xx} vs B_{tilted} in the top panel and vs $B_\perp = B_{tilted} \cos \theta$ in the bottom panel. According to parameters and set-up of Mani's experiment, we have used a confinement in z of 30 nm and MW frequency of 63 GHz. We present different curves corresponding to different tilt angles (θ). θ values are: $\theta = 0^0, 60^0, 70^0, 80^0$. In this case $B_{||} = B_{tilted} \sin \theta$. In the top panel we present calculated curves for each θ in individual panels. We observe MIRO displacement at larger B_{tilted} for increasing values of θ . This is explained considering that $B_\perp = B_{tilted} \cos \theta$ and that peak positions are only governed by B_\perp . In the bottom panel we can see all curves together for comparison. We observe, as in experiment, how the quenching effect is not uniform and more intense with increasing values of B_{tilted} and θ .

Our model explains this peculiar behavior with the expression of $B_{||}$ and equations (5) and (6). Increasing values of B_{tilted} and θ give rise to an increasing damping according to equation (5) and decreasing A and MIRO according to equation (6). Thus, we observe a soft quenching for small values of B_\perp and θ , and it gets progressively more important for larger values of them. This feature is shown in the inset of Fig. 4 bottom panel, where we present the peak resistance vs $\cos \theta$ for peaks= 1, 2, 3, as in experiment²³. The decrease in the peak resistance is larger for peak 1 than for peaks 2, 3 as θ increases. These results are in good agreement with Mani's experiment²³.

In summary, we have presented a theoretical model on the effect of an in-plane magnetic field on MIRO and ZRS in 2DES. Experimental results show different behaviors depending on the set-up of the magnetic field. In an independent $B_{||}$ experiments report a clear quenching of MIRO and ZRS. In a tilted B , experiments show oscillations displacement and an unbalanced quenching. We have presented a theoretical model which explains these results based in a common physical mechanism. The MW-driven oscillating electronic orbit motion is increasingly damped by the presence of $B_{||}$. The understanding of this behavior will allow to control the transport properties in a MW irradiated Hall bar. In particular MIRO and ZRS features by tuning external magnetic fields in different configurations.

This work has been supported by the MCYT (Spain) under grant MAT2005-0644 and by the Ramón y Cajal program.

-
- ¹ J. Iñarrea, G. Platero and C. Tejedor, *Semicond. Sci. Tech.* **9**, 515, (1994); *Phys. Rev. B*, **51**, 5244, (1995); *Europhys. Lett.* **34**, 43, (1996).
- ² R. G. Mani, J. H. Smet, K. von Klitzing, V. Narayana-murti, W. B. Johnson, V. Umansky, *Nature* **420** 646 (2002).
- ³ M. A. Zudov, R. R. Du, N. Pfeiffer, K. W. West, *Phys. Rev. Lett.* **90** 046807 (2003).
- ⁴ S. A. Studenikin, M. Potemski, A. Sachrajda, M. Hilke, L. N. Pfeiffer, K. W. West, *Phys. Rev. B* **71**, 245313 (2005).
- ⁵ J. Iñarrea and G. Platero, *Phys. Rev. Lett.* **94** 016806, (2005); J. Iñarrea and G. Platero, *Phys. Rev. B* **72** 193414 (2005).
- ⁶ A. C. Durst, S. Sachdev, N. Read, S. M. Girvin, *Phys. Rev. Lett.* **91** 086803 (2003).
- ⁷ C. Joas, J. Dietel and F. von Oppen, *Phys. Rev. B* **72**, 165323, (2005).
- ⁸ X. L. Lei, S. Y. Liu, *Phys. Rev. Lett.* **91**, 226805 (2003); X. L. Lei, *Appl. Phys. Lett.* **90**, 132119 (2007).
- ⁹ V. Ryzhii and V. Vyurkov, *Phys. Rev. B* **68** 165406 (2003).
- ¹⁰ P. H. Rivera and P. A. Schulz, *Phys. Rev. B* **70** 075314 (2004).
- ¹¹ Manuel Torres and Alejandro Kunold, *Phys. Rev. B* **71**, 115313 (2005).
- ¹² R. L. Willett, L. N. Pfeiffer and K. W. West, *Phys. Rev. Lett.* **93**, 026804, (2004).
- ¹³ A. A. Bykov, D. R. Islamov, D. V. Nomokonov, A. K. Bakarov, *JETP LETTERS*, **86**, 608-611, (2008).
- ¹⁴ J. Iñarrea and G. Platero, *Appl. Phys. Lett.*, **89**, 052109, (2006).
- ¹⁵ M. A. Zudov, R. R. Du, N. Pfeiffer, K. W. West, *Phys. Rev. Lett.* **90** 046807 (2003).
- ¹⁶ J. Iñarrea and G. Platero, *Appl. Phys. Lett.* **89**, 172114, (2006).
- ¹⁷ J. H. Smet, B. Gorshunov, C. Jiang, L. Pfeiffer, K. West, V. Umansky, M. Dressel, R. Dressel, R. Meisels, F. Kuchar, and K. von Klitzing, *Phys. Rev. Lett.* **95**, 116804 (2005).
- ¹⁸ J. Iñarrea and G. Platero, *Phys. Rev. B*, **76**, 073311, (2007); J. Iñarrea, *Appl. Phys. Lett.* **90**, 172118, (2007); J. Iñarrea, *Appl. Phys. Lett.* **90**, 262101, (2007).
- ¹⁹ S. Wang and T. Ng, *Phys. Rev. B* **77**, 165324 (2008).
- ²⁰ S. A. Studenikin, A. S. Sachrajda, J. A. Gupta, Z. R. Wasilewski, O. M. Fedorych, M. Byszewski, D. K. Maude, M. Potemski, M. Hilke, K. W. West and L. N. Pfeiffer, *Phys. Rev. B*, **76**, 165321, (2007).
- ²¹ J. Iñarrea, *Appl. Phys. Lett.* **92**, 192113 (2008).
- ²² C. L. Yang, R. R. Du, L. N. Pfeiffer and K. W. West, *Phys. Rev. B*, **74**, 045315, (2006).
- ²³ R. G. Mani, *Phys. Rev. B*, **72**, 075327, (2005); R. G. Mani, *Appl. Phys. Lett.*, **92**, 102107, (2008).
- ²⁴ J. C. Maan, *Two Dimensional systems, Heterostructures and Superlattices* p.183. Springer Verlag Berlin (1984).
- ²⁵ R. Merlin, *Sol. Stat. Comm.*, **64**, 99, (1987).
- ²⁶ V. Fock, *Z. Phys.* **47**, 466 (1928); C.G. Darwin, *Proc. Cam-*

bridge Philos. Soc. **27**, 86, (1930).
²⁷ B. K. Ridley. *Quantum Processes in Semiconductors*, 4th

ed. Oxford University Press, (1993).